UIR-band emission from M supergiants

R. J. Sylvester,[1] M. J. Barlow[1] and C. J. Skinner[2]
[1]*Department of Physics and Astronomy, University College London, Gower Street, London WC1E 6BT*
[2]*Institute for Geophysics and Planetary Physics, Lawrence Livermore National Laboratory,*
7000 East Avenue, L-413, Livermore, CA 94550, USA

ABSTRACT
We have obtained 10-μm spectra of 16 M supergiants, 15 of them in the h and χ Per association. All of the stars exhibit silicate emission features, but in addition seven of the stars show narrow UIR (unidentified infrared) band emission features, at 11.3 μm, 8.65 μm and other wavelengths, which are normally associated with carbon-rich media. Not only are these the coolest objects to have been found to exhibit UIR-band emission, but the outflows from these classical oxygen-rich stars should form only O-rich particles according to equilibrium condensation theory. We interpret our results in terms of the non-equilibrium chemistry model by Beck et al., whereby chromospheric UV radiation can liberate some atomic carbon via the photodissociation of CO molecules, enabling the formation of carbon-rich species as well as silicates. Such a chromospheric UV radiation field could also provide the photons needed to excite the observed UIR-band emission.

Key words: molecular processes – circumstellar matter – supergiants – dust, extinction – infrared: stars.

1 INTRODUCTION

According to the standard scenario for dust grain formation around cool stars (e.g. Gilman 1969), the great stability of gaseous CO should lead to the less abundant of the elements carbon and oxygen being locked up by that molecule, so that only oxygen-rich grains should form in environments where C/O<1, by number, while only carbon-rich grains should condense when C/O>1. Observations have largely confirmed this scenario, although a number of apparent exceptions have been found. Carbon stars have been found whose *IRAS* Low Resolution Spectrometer (LRS) spectra exhibit silicate emission features (Willems & de Jong 1986; Skinner, Griffin & Whitmore 1990; Lloyd-Evans 1990) – all these objects have been found to be J-type carbon stars, whose optical spectra exhibit high $^{13}C/^{12}C$ ratios. Skinner & Whitmore (1988b) and Skinner et al. (1990) discussed two oxygen-rich M supergiants, AD Per and MZ Cas, whose LRS spectra appeared to show the 11.5-μm silicon carbide emission feature, in addition to the silicate emission feature. As part of a survey of the mid-infrared spectral characteristics of circumstellar dust around cool evolved stars, we have obtained higher resolution 10-μm spectra of these two stars, and of 14 further M supergiants in the h and χ Per association. These spectra reveal that emission features arising from carbon-rich material are indeed present in the 10-μm spectra of a number of M supergiants, although we conclude that the carbon-rich material is not silicon carbide but is instead composed of hydrocarbons of the polycyclic aromatic hydrocarbon or hydrogenated amorphous carbon type.

2 OBSERVATIONS

All the stars were observed on the nights of 1992 October 4–7 using the United Kingdom Infrared Telescope (UKIRT) with the common-user spectrometer CGS3, a 10- and 20-μm grating spectrometer built at University College London. CGS3 contains an array of 32 discrete As:Si photoconductive detectors, and three interchangeable, permanently mounted gratings covering the 7.5–13.5 and 16.0–24.5 μm wavebands. Two grating settings give a fully sampled 64-point spectrum of the chosen waveband. We obtained 7.7–13.3 μm spectra with a 5.5-arcsec circular beam, yielding a spectral resolution of 0.17 μm. Wavelength calibration was with respect to observations of a Kr arc-lamp. The telescope secondary was chopped east–west at 5 Hz using a 30-arcsec throw. We observed 15 M-type supergiants in the h and χ Per association, 14 chosen from the list of Cohen & Gaustad (1973), plus XX Per, an M3.6Ib supergiant listed by Humphreys (1978) as being in the same association. In addition, the M1.3Iab supergiant MZ Cas was observed since, as noted above, its *IRAS* LRS spectrum had been found by Skinner & Whitmore (1988b) to be similar to that of AD Per in appearing to show an 11.5-μm silicon carbide feature.

Five stars, α Tau, α Cet, β Peg, ε Cyg and α Aur, were used as standards, and sky spectra obtained using a rotating sector chopper were used for flat-fielding all spectra. The spectra of sources taken using α Tau as the standard star were flux-calibrated using the absolutely calibrated spectrum of α Tau constructed by Cohen, Walker & Witteborn (1992), whilst some sources were calibrated using a similarly constructed

Table 1. The programme stars.

Source	Spectral Type	K	F_{12} (Jy)	1992 Date	$\frac{F_{10,obs}}{F_{10,cont}}$	λ_{max} (μm)	FWHM (μm)	$\dot{M}$ ($M_\odot yr^{-1}$)	$EW_{11.3}$ (Å)	$I(11.3)$ (W m^{-2})	$\frac{I(8.65)}{I(11.3)}$
S Per	M4.5Iab	1.45	329.5	Oct 4	4.0	9.7	3.3	5.9×10^{-5}	<100		
SU Per	M3.3Ib	1.39	45.1	Oct 4	3.7	10.0	2.7	5.2×10^{-6}	<100		
RS Per	M4.4Ib	1.63	68.3	Oct 6	3.8	9.8	2.6	1.0×10^{-5}	<100		
XX Per	M3.6Ib	1.83	57.1	Oct 6	2.6	9.7	2.5	7.9×10^{-6}	<100		
HD 14826	M3.1Ib	1.94	18.1	Oct 7	1.5	10.6	$\geq$3.8	4.2×10^{-7}	210	1.0×10^{-14}	
YZ Per	M1.9Ia	2.03	32.9	Oct 7	4.7	9.8	2.4	6.6×10^{-6}	<100		
AD Per	M2.4Iab$^-$	2.06	20.3	Oct 4	1.9	10.4	3.1	1.3×10^{-6}	320	1.5×10^{-14}	0.28
KK Per	M1.9Ib	2.13	17.6	Oct 7	1.8	10.3	3.4	1.2×10^{-6}	610	2.8×10^{-14}	0.64
BU Per	M3.7Ib	2.24	39.8	Oct 4	6.1	9.9	2.5	9.3×10^{-6}	<100		
HD 14404	M0.7Iab	2.34	12.0	Oct 7	1.7	10.5	$\geq$3.8	3.3×10^{-7}	210	0.6×10^{-14}	0.67:
FZ Per	M0.3Iab$^-$	2.53	10.7	Oct 7	1.7	10.9	3.3	2.9×10^{-7}	380	1.1×10^{-14}	0.77
HD 14242	M5.7Iab	2.56	11.8	Oct 7	1.5	10.8	3.7	2.2×10^{-7}	380	1.1×10^{-14}	0.55:
T Per	M2.1Iab	2.58	9.7	Oct 4	1.5	10.4	3.6	9.2×10^{-8}	<100		
BD+56°595	M5.8Iab	2.80	7.5	Oct 7	1.1	~11.3	~3.3	$\geq10^{-8}$	?		
HD 13658	M5.4Iab	3.21	3.3	Oct 7	1.2	~10.8	~3.1	$\geq10^{-8}$	?		
MZ Cas	M1.3Iab	2.65	20.6	Oct 7	1.7	9.9	3.0	2.4×10^{-6}	350	1.7×10^{-14}	0.77

β Peg spectrum provided by M. Cohen (1992, private communication). The other spectra were calibrated with respect to α Cet, ε Cyg and α Aur, which were assumed to emit as blackbodies in the 10-μm region, with effective temperatures of 3730, 4790 and 4880 K and 10.0-μm fluxes of 226.7, 40.5 and 228.8 Jy, respectively. The blackbody assumption is likely to be reasonable for the 10-μm region of the G5III standard α Aur, but the possible presence of SiO absorption bands between 8 and 9 μm in the spectra of the standards α Cet (spectral type M2III) and ε Cyg (spectral type K0III) was cause for concern. We tested the blackbody assumption by normalizing the Cohen spectrum of β Peg, which has a similar spectral type (M2.5II–III), to the 10.0-μm flux of α Cet, and then calibrated the target spectra with this synthetic 'standard'. The discrepancy between the spectra reduced in this fashion and those reduced by treating the standard as a blackbody was found to have a peak value of approximately 8 per cent, occurring at 8 μm.

Two stars, RS Per and BD+56°595, were observed through broken cloud. This meant that some of the 10-s integration cycles were obtained whilst the source was obscured by cloud. However, by monitoring the integrated flux level for each cycle, we were able to determine which were the most badly affected cycles, and were then able to discard them. It is possible that the 7.5–13 μm slopes of the spectra obtained for these two objects could differ from the true slopes, if there were some residual thin cloud present with non-grey extinction.

Table 1 lists the stars observed. Spectral types are taken from White & Wing (1978). Table 1 also lists K (2.18 μm) magnitudes for the stars, from Johnson (1966), along with their colour-corrected *IRAS* 12-μm fluxes. The colour-correction factors were obtained by convolving the CGS3 spectra with the *IRAS* 12-μm band spectral response curve (*IRAS* Explanatory Supplement) to give the 12-μm in-band flux. This in-band flux was then used to derive a nominal 12.0-μm flux, making the normal λ^{-1} spectral assumption used for the *IRAS* Point Source Catalog. Comparison of this flux with the actual 12.0-μm flux in the CGS3 spectrum allowed us to obtain the colour-correction factor for each star, which was then used to correct the published *IRAS* 12-μm flux. The derived colour-correction factors all lie in the range 1.03–1.24.

3 RESULTS

The calibrated CGS3 spectra are displayed in Figs 1(a)–(p), along with the colour-corrected *IRAS* 12-μm fluxes (filled circles). Due to imperfect cancellation of the time-varying atmospheric ozone band, the error bars of the CGS3 spectra are larger at approximately 9.6 μm, whilst the larger error bars associated with the first few points in each spectrum are due to the high opacity at the short-wavelength edge of the 10-μm atmospheric window. The two shortest-wavelength points of each spectrum were discarded due to the high noise levels, and hence the spectra presented in Figs 1 and 2 contain only 62 points. There is very good agreement between the 12.0-μm flux levels of the calibrated CGS3 spectra and the *IRAS* 12-μm photometry, with the only sources for which there is substantial disagreement being RS Per and BD+56°595, the two sources that were observed through broken cloud. The dashed lines in Fig. 1, which are normalized to the 8-μm region of each spectrum, are blackbody functions corresponding to the effective temperatures listed as a function of spectral type by Schmidt-Kaler (1982; these were between 2700 and 3600 K). The normalized blackbody functions were found also to pass through the K-band continuum fluxes corresponding to the photometry listed in column 3 of Table 1 [a zero-magnitude K-band (2.18-μm) flux of 655.5 Jy was adopted]. Apart from RS Per and BD+56°595, the exception to this was S Per, whose 7.5–8 μm 'continuum' lies well above a 'photospheric' 2900-K blackbody extrapolated from 2.18 μm. A blackbody of 750 K was found to give a good fit to the observed 3–8 μm excess of S Per after subtraction of a 2900-K blackbody normalized to 2.18 μm. The sum of the 2900- and 750-K blackbody spectra is
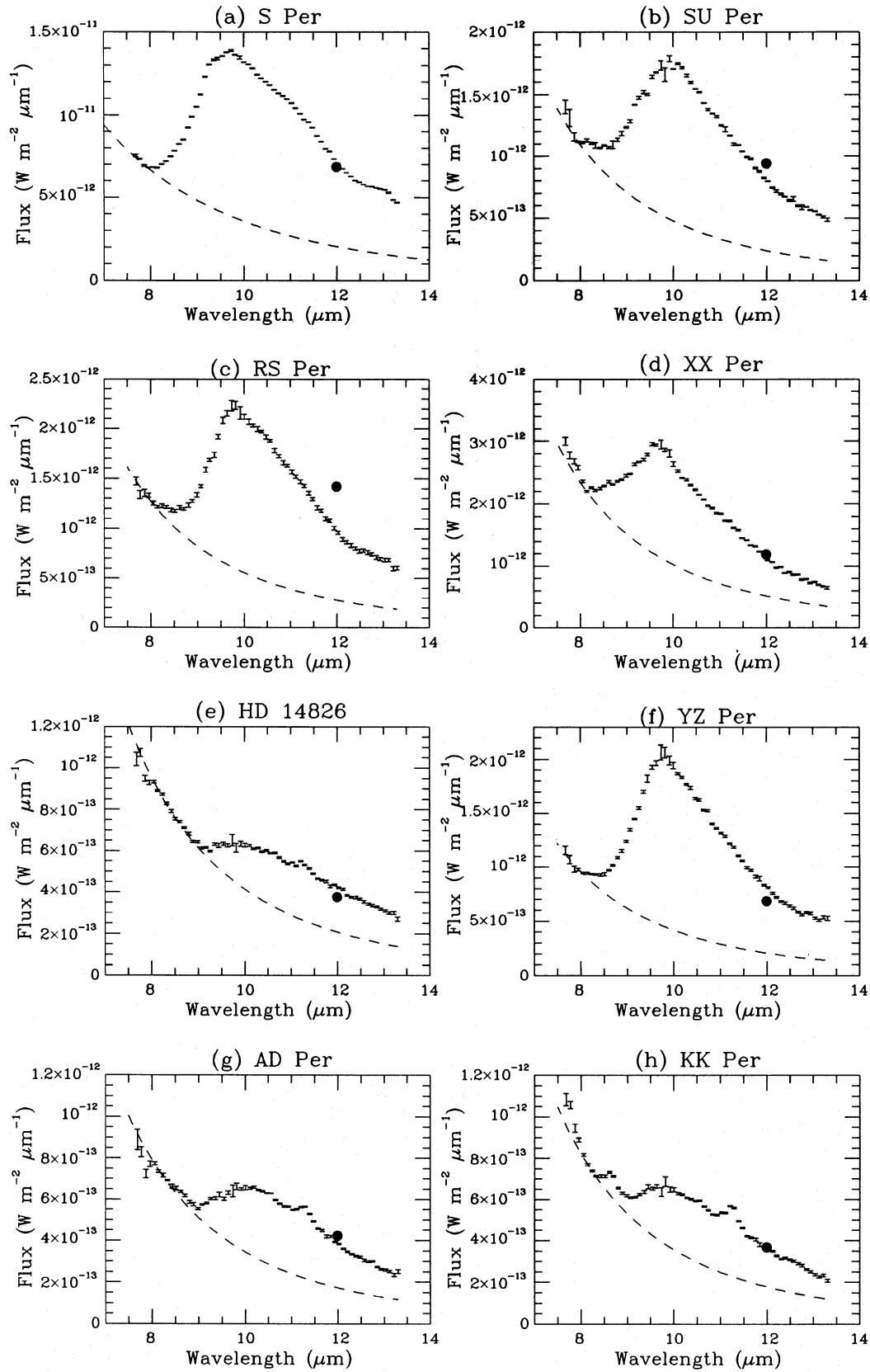
Figure 1. CGS3 spectra of M supergiants. Error bars: observed spectrum; dashed line: normalized blackbody continuum (see text); filled circles: colour-corrected *IRAS* 12-μm fluxes.
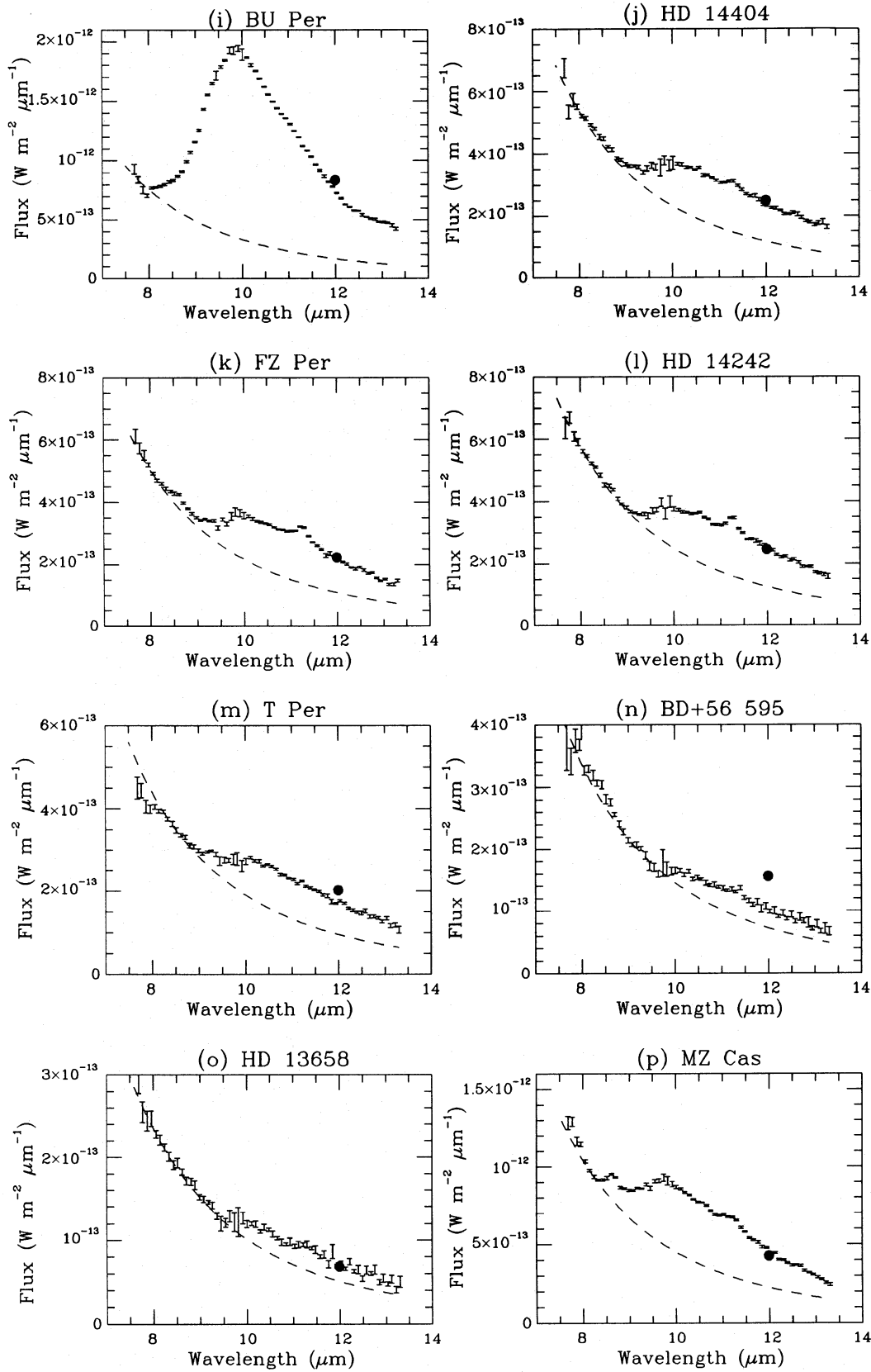
Figure 1 – *continued*

plotted as the dashed line in Fig. 1(a). It should be noted that the long-wavelength ends of the spectra displayed in Fig. 1 all lie well above the extrapolated blackbody continua. Laboratory silicate emissivities normally fall to very low values longwards of 13 μm (e.g. Kratschmer & Huffman 1979) and, although astronomical silicate emissivities have been proposed for which the emissivity trough between the 10- and 18-μm features does not fall to such low values (e.g. Draine & Lee 1984), these emissivities are themselves based partly upon the spectra of sources similar to those presented here. Skinner & Whitmore (1987, 1988b) have attributed a large fraction of the mid-infrared continuum emission observed from M supergiants such as α Ori and S Per to chromospheric free–free emission. However, for the purposes of this paper we have not modelled the contribution made by chromospheric free–free emission to the mid-infrared continuum of each star.

The spectra of the more luminous sources, such as S Per and SU Per, show large amounts of excess emission, due to a strong silicate feature, as is often observed in the spectra of M supergiants. The fainter sources show a weaker silicate feature, but in addition a number of narrow emission features are present. The 'excess' spectra (i.e. after subtraction of the normalized blackbodies) of six of the sources that displayed these features – MZ Cas, KK Per, AD Per, HD 14404, HD 14242 and FZ Per– are displayed in Fig. 2. The peak wavelengths and FWHM of the various narrow features were determined by subtracting a smooth continuum, representing the underlying silicate emission, and fitting Gaussian profiles to the features using the ELF suite of subroutines, written by Dr P.J. Storey, within the Starlink package DIPSO (Howarth & Murray 1991). The strongest of the features, at approximately 11.3 μm, was well-defined in all six spectra, with a central wavelength varying between 11.23$\pm$0.03 and 11.31$\pm$0.04 μm, and a FWHM of between 0.27$\pm$0.08 and 0.32$\pm$0.06 μm. A feature at approximately 8.65 μm is most obvious in the excess spectra of MZ Cas, KK Per and FZ Per, but can be seen in all six sources, despite the presence of significant noise in the excess spectra of HD 14404 and HD 14242. The peak wavelength of this feature was found to lie between 8.62 and 8.66 μm. The width of the feature was not well-constrained in most cases, but FWHM values of 0.17$\pm$0.06 μm (i.e. unresolved) and 0.26$\pm$0.07 μm were obtained for MZ Cas and KK Per, respectively.

A weak emission feature at about 10.6 μm is most evident in the spectrum of HD 14242, where it stands out clearly above the broad underlying silicate profile. In some of the other spectra, notably those of HD 14404 and KK Per, the feature appears at first glance to be confined to just a couple of data points with slightly enhanced fluxes. However, a close inspection of the spectra of AD Per and KK Per reveals that there is a definite change in the spectral slope between those points immediately shortward of the 'isolated' maximum point, and those longward of it. To investigate the possibility that the 10.6-μm feature was an artefact produced by the instrument or by the data-reduction process, we inspected the spectra of the standard stars, as well as those of other objects observed on the same nights. No indication was found of a 10.6-μm absorption feature in the raw spectra of the standards, or of 10.6-μm emission features in the spectra of oxygen-rich asymptotic giant branch (AGB) stars observed on the same nights; we conclude therefore that the 10.6-μm emission is a real feature in the spectra of the M supergiants shown in Fig. 2. Measurements of the peak wavelength of the feature gave values ranging from 10.53$\pm$0.02 to 10.61$\pm$0.01 μm, with their FWHM ranging from 0.17$\pm$0.05 μm (unresolved) to 0.33$\pm$0.08 μm.

A fourth feature is detected in the excess spectra, at approximately 12.6 μm. Again, this is a weak feature; it is readily seen in the spectra of HD 14404 and MZ Cas but is not as clearly present in the spectra of the other four stars in Fig. 2.

Table 1 also gives measurements of the strengths of the silicate and UIR-band features. The silicate contrast, $F_{10,obs}/F_{10,cont}$, is defined as the ratio of the observed flux at 10.0 μm to that of the underlying blackbody continuum normalized at 8 μm, also measured at 10.0 μm. The derived silicate contrasts are listed in column 6 of Table 1; column 7 lists λ_{max}, the wavelength at which each silicate excess flux distribution peaks; and column 8 lists the FWHM measured for each silicate excess flux distribution. Mass-loss rates for the stars are given in column 9. These were derived by applying the method of Skinner & Whitmore (1988a) to the current CGS3 data, using a distance of 2.3 kpc for the h and χ Per stars and a distance of 2.9 kpc for MZ Cas (Humphreys 1978). The strength of the 11.3-μm band was determined by measuring its equivalent width with respect to the underlying photospheric plus silicate emission. The derived values of EW(11.3) are listed in column 10 of Table 1, while column 11 of Table 1 lists the integrated flux in the 11.3-μm feature. Finally, column 12 of Table 1 lists the ratio of the integrated fluxes in the 8.65- and 11.3-μm features, $I(8.65)/I(11.3)$, for those stars where both features are reasonably well-defined.

4 DISCUSSION

We associate the narrow emission features in Fig. 2 with the unidentified infrared (UIR) bands. These are usually attributed to hydrocarbon vibrational modes in species such as hydrogenated amorphous carbon (HAC; Duley & Williams 1981) or polycyclic aromatic hydrocarbons (PAHs; Léger & Puget 1984). Both AD Per and MZ Cas, the objects whose *IRAS* LRS spectra appear to show the SiC feature in emission (Skinner & Whitmore 1988b), exhibit narrow UIR bands in their CGS3 spectra. The lower spectral resolution and poorer signal-to-noise ratio of the LRS spectra seem to have resulted in the blending of the narrow 11.3-μm UIR band and the silicate feature, making it appear that a broad SiC feature is present.

The 11.3-μm UIR-band feature has been associated with out-of-plane C–H bending modes, versus in-plane bending modes for the 8.65-μm feature (Allamandola, Tielens & Barker 1989). Allamandola et al. attribute a 12.7-μm feature sometimes discerned in astronomical UIR-band spectra to a C–H out-of-plane bending mode of triply adjacent H-atoms – the feature peaking at about 12.6 μm seen in several of our spectra in Fig. 2 appears to be the same feature. The 10.6-μm emission peak seen in several of our spectra is probably the same feature as the 10.6–10.75 μm band first detected by Justtanont, Barlow & Skinner (1993) in CGS3 spectra of a number of carbon-rich F- and G-type post-AGB objects that had been found by Kwok, Volk & Hrivnak (1989) to exhibit a 21-μm emission band in their *IRAS* LRS spectra. We note that a feature at about 10.5 μm is evident amongst the transitions of PAHs such as chrysene, pyrene and coronene that are illustrated in fig. 1 of Allamandola et al. (1989).

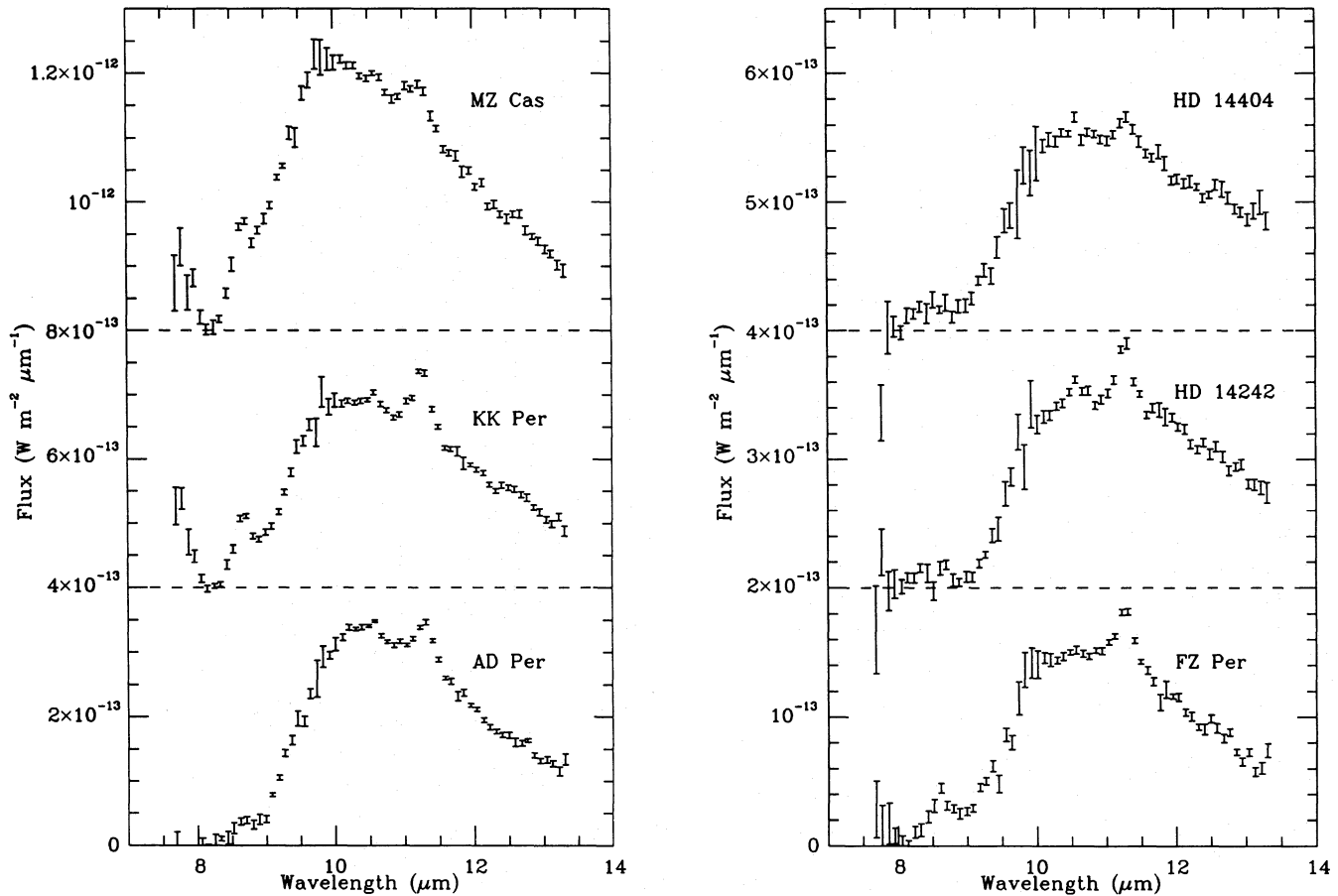**Figure 2.** 'Excess' spectra after subtraction of blackbodies which were normalized to the flux at 8 μm (see text).

Among the family of UIR-band features, a strong feature attributed to aromatic C–C stretching modes is usually prominent at 7.6–8.0 μm (Allamandola et al. 1989). Because of our choice of 8.0 μm for the normalization of the steeply rising stellar continuum, and the effect of the short-wavelength atmospheric cut-off, such a feature is difficult to identify positively in our spectra. However, it is noticeable that the two stars with the most prominent 8.65-μm bands, namely KK Per and MZ Cas, appear to show excess emission shortwards of 8 μm (Figs 1 and 2).

A CGS3 10-μm spectrum of AD Per had been obtained by us on 1990 October 6 (reproduced by Barlow 1993), and agrees with the 1992 October 4 spectrum shown in Figs 1 and 2. Because of the lack of a prominent 8.65-μm emission feature in AD Per's spectrum, we had entertained the possibility that the 11.3-μm band in the spectrum of AD Per might be attributable to crystalline olivine, as had been proposed by Bregman et al. (1987) and Campins & Ryan (1989) for a similar narrow emission feature seen superposed on a broad silicate feature in the spectrum of Comet P/Halley. However, the clear presence of the 8.65-μm UIR band in the spectra of a number of the other M supergiants that show the 11.3-μm feature, such as MZ Cas and KK Per, led us to abandon this interpretation, since none of the crystalline olivine spectra illustrated by Campins & Ryan exhibits a feature near this wavelength. In view of the fact that carbonaceous emission

features peaking at about 3.36 μm were clearly present in the spectrum of Comet Halley (Baas, Geballe & Walther 1986; Knacke, Brooke & Joyce 1987), we suggest that a UIR-band contribution to Comet Halley's 11.3-μm feature should be taken into account.

An explanation must be sought for the strange combination, in a significant number of the M supergiant 10-μm spectra, of silicate emission (normally indicative of oxygen-rich material) and UIR-band emission (normally indicative of carbon-rich material). One possibility is that the UIR-band emission does not arise from the stars themselves, but from material distributed in surrounding nebulosity. Nebulae exhibiting UIR-band emission as strong as that seen here are normally very bright, whereas there is no obvious nebulosity to be seen in the environs of h and χ Per. Further, a plot of the positions of the h and χ Per M supergiants reveals no spatial correlation between the stars that exhibit UIR-band emission. Finally, the fact that all the stars were observed by chopping between object and reference beams separated by 30 arcsec on the sky implies that, if the UIR-emitting material were distributed independently of the M supergiants, the features should have appeared equally often in the object and reference beams, so that UIR bands in apparent absorption should occasionally have been seen, which was not the case. We conclude that the UIR-band emission originates from the same stellar outflows as do the silicate emission features.

Equilibrium theories of dust formation do not predict the presence of carbon-rich particles in the winds of classical oxygen-rich objects such as M supergiants. Such stars are expected to have C/O ratios close to or less than solar, so that only silicates and other oxygen-rich materials should condense if CO molecules were locking up most carbon atoms. The chemical equilibrium condensation calculations of Sharp (1989) showed that weakly oxygen-rich mixtures, namely those with initial C/O ratios larger than about 0.83, could have sufficient oxygen removed from the gas phase by oxide and silicate condensation that the remaining gas becomes carbon-rich, enabling the formation of hydrocarbons and carbon particles. However, this scenario is not expected to be applicable to environments such as M supergiant winds, whose C/O ratios should be solar (0.5) or less. Unlike AGB stars, dredge-up to the surface of carbon synthesized in helium-burning layers is definitely not predicted for the massive stars that evolve into M supergiants. If anything, their C/O ratios are expected to be less than solar, due to the exposure of CN- and CNO-cycle-processed material at the surface by the effects of convective dredge-up and prior mass-loss stripping. For example, Lambert et al. (1984) derived a C/O ratio of 0.4 for the M2Iab supergiant α Ori. The optical photospheric spectrum of AD Per, one of the M supergiants exhibiting UIR-band emission, shows no sign of carbon species (Skinner et al. 1990).

A possible explanation for the simultaneous presence of oxygen-rich and carbon-rich particles in the outflows from O-rich M supergiants is provided by the work of Beck et al. (1992), who carried out non-equilibrium chemistry calculations for oxygen-rich circumstellar flows. They found that strong ultraviolet emission from a warm chromosphere can cause a departure from chemical equilibrium due to the photodissociation of CO molecules. This produces a population of free carbon atoms, a situation not allowed under the assumption of chemical equilibrium, and they predicted that this could enable the formation of carbon dust alongside the expected oxygen-rich silicate dust. Species containing nitrogen were not included in the chemical reaction network of Beck et al., but presumably the photodissociation of CN molecules, whose abundance may be enhanced by the mixing up of nitrogen from material processed by the CNO cycle, would also aid the formation of carbon particles. Since hydrogen is predicted by Beck et al. to be in the atomic form, a reasonable degree of surface hydrogenation should occur for any carbon particles that are formed. Finally, chromospheric emission may also provide the UV photons that are thought to be required to stimulate UIR-band emission from PAHs or similar carbonaceous species (Allamandola et al. 1989).

In the context of this model for the origin of the observed UIR-band emission, there are a number of possible reasons as to why not all the M supergiants in our sample exhibit detectable UIR bands. Among the h and χ Per supergiants, UIR-band emission is not detected from any stars with *IRAS* 12-μm fluxes larger than 21 Jy or lower than 10 Jy, but is detected from all the stars with fluxes within these limits. The two faintest stars in our sample, BD+56°595 and HD 13658, have significantly weaker silicate excesses (Figs 1n and 1o) than any of the other stars – the lower signal-to-noise ratios of their CGS3 spectra leave open the possibility that UIR-band emission could be present at the same contrast as in the excess spectra shown in Fig. 2. However, any 11.3-μm band emission from T Per is at least three times weaker than that

from FZ Per and HD 14242. Since no UIR-band emission was detected from any of the three stars in Table 1 with mass-loss rates equal to or below the 9×10^{-8} M$_\odot$ yr^{-1} derived for T Per, one might envisage that any C atoms liberated by the UV photodissociation of CO are present at such low number densities that they fail to associate into carbon species in sufficiently large numbers to yield detectable UIR-band emission.

The six stars brighter than 21 Jy at 12 μm (Table 1 and Fig. 1) possess such strong silicate features that the equivalent width of the 11.3-μm feature would be below the upper limits listed in Table 1 if 11.3-μm band emission were present at the same flux levels, $I(11.3)$, listed in Table 1 for all but one of the h and χ Per supergiants with detected 11.3-μm bands. However, KK Per has a very strong 11.3-μm band flux which would have been easily detectable if it had been emitted by SU Per, YZ Per or BU Per. Another possible reason for the absence of UIR-band emission from the stars with the strongest silicate bands therefore suggests itself. Since the strength of the silicate band is believed to be proportional to the mass-loss rate (Skinner & Whitmore 1988a), these stars may have sufficiently large dust columns that they are optically thick to any chromospheric UV photons emitted underneath. This could lead to a failure to liberate carbon via photodissociation of CO and/or an inability to excite any emission from PAH-type particles that might exist. In this regard, it is noteworthy that none of the M supergiants in Table 1 with derived mass-loss rates in excess of 5×10^{-6} M$_\odot$ yr^{-1} exhibits UIR-band emission, whereas all the supergiants whose derived mass-loss rates lie between 2×10^{-7} and 1.3×10^{-6} M$_\odot$ yr^{-1} *do* exhibit UIR-band emission. We note that, since the method of Skinner & Whitmore (1988a) makes use of the strength of the silicate feature at 9.8 μm relative to a baseline between 7.9 and 13.3 μm, as originally defined for classification in the *IRAS* LRS catalogue, the mass-loss rates of these stars could be somewhat underestimated, due to their silicate features peaking at, and extending to, longer wavelengths than do the silicate features of the brighter stars (see below). The incidence of UIR-band emission amongst M supergiants with mass-loss rates in the range $(1-5) \times 10^{-6}$ M$_\odot$ yr^{-1} is less certain. MZ Cas exhibits 8.65- and 11.3-μm UIR-band emission, and has a mass-loss rate of 2.4×10^{-6} M$_\odot$ yr^{-1} according to Table 1. On the other hand, the mid-infrared spectrum of α Ori published by Treffers & Cohen (1974) did not reveal UIR-band emission at 11.3 μm or elsewhere, and yields a mass-loss rate of 1.1×10^{-6} M$_\odot$ yr^{-1} for a distance of 200 pc. However, since they are at different distances, a comparison of the mass-loss rates of these two stars with those in h and χ Per is less reliable than considering only the relative values of the mass-loss rate for the h and χ Per stars, which are all at effectively the same distance.

All of the h and χ Per stars with *IRAS* 12-μm fluxes less than 21 Jy appear to have similar silicate feature profiles, their excess flux profiles peaking between 10.3 and 10.9 μm, with a FWHM of between 3.0 and 3.9 μm (see Fig. 3 and columns 8 and 9 of Table 1). On the other hand, the stars with 12-μm fluxes exceeding 21 Jy, none of which exhibits the narrow UIR-band features, have silicate profiles differing notably in shape and width from those of the fainter stars, their excess flux profiles being similar to each other and peaking between 9.7 and 10.0 μm, with a FWHM of between 2.4 and 2.7 μm (see Fig. 4 and Table 1), apart from the extreme object S Per,
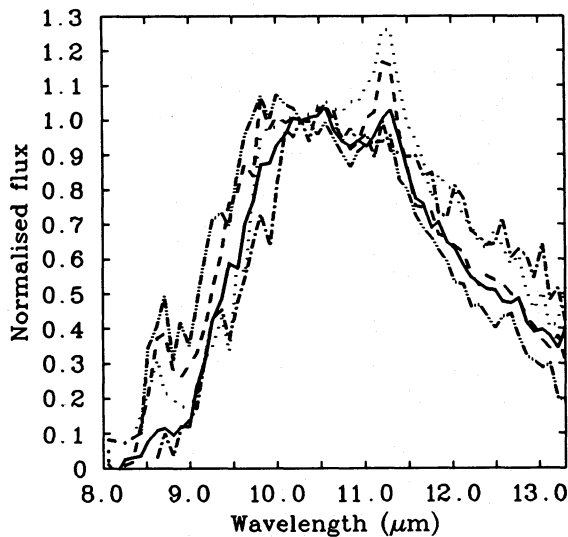
Figure 3. Excess flux profiles for stars with *IRAS* 12-μm fluxes less than 21 Jy: AD Per (solid line), KK Per (dashed line), FZ Per (dotted line), T Per (dash-dotted line), MZ Cas (dash-double-dotted line). The spectra are normalized to unity at 10.3 μm.
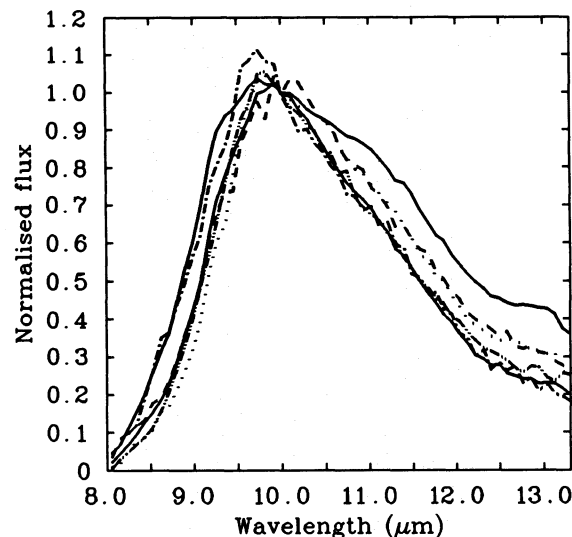

Figure 4. Excess flux profiles for stars with *IRAS* 12-μm fluxes greater than 21 Jy: S Per (upper solid line), SU Per (dashed line), RS Per (dotted line), XX Per (dash-dotted line), YZ Per (dash-double-dotted line), BU Per (lower solid line). The spectra are normalized to unity at 10.0 μm.

that, during the same nights that the current M supergiants were observed, we obtained 10-μm CGS3 spectra of 60 O-rich AGB stars, including seven classified by LML as having 'broad' features, but none was found to exhibit narrow emission features at 11.3 μm or elsewhere.

A shift to shorter wavelengths of the silicate peak is indicative of a decreasing silicate Mg/Si ratio, with enstatites, $(Fe_nMg_{1-n})SiO_3$, peaking at shorter wavelengths than olivines, $(Fe_nMg_{1-n})_2SiO_4$ (Day & Donn 1978; Stephens & Russell 1979). Enstatites have somewhat lower condensation temperatures than do olivines (Tielens 1990), implying that they should form at larger radii than do olivines and thus, if the critical densities for condensation are similar, that higher mass-loss rates are needed for significant enstatite formation. The observed shift of the M supergiant excess flux peak to shorter wavelengths with increasing mass-loss rate is consistent with this expectation.

REFERENCES

Allamandola L. J., Tielens A. G. G. M., Barker J. R., 1989, ApJS, 71, 733
Baas F., Geballe T. R., Walther D. M., 1986, ApJ, 311, L97
Barlow M. J., 1993, in Kwok S., ed., ASP Conf. Ser. 41, Astronomical Infrared Spectroscopy: Future Observational Directions. Astron. Soc. Pac., San Francisco, p. 97
Beck H. K. B., Gail H.-P., Henkel R., Sedlmayr E., 1992, A&A, 265, 626
Bregman J. D., Campins H., Witteborn F. C., Wooden D. H., Rank D. M., Allamandola L. J., Cohen M., Tielens A. G. G. M., 1987, A&A, 187, 616
Campins H., Ryan E. V., 1989, ApJ, 341, 1059
Cohen M., Gaustad J. E., 1973, AJ, 186, L131
Cohen M., Walker R. G., Witteborn F. C., 1992, AJ, 104, 2030
Day K. L., Donn B., 1978, ApJ, 222, L45
Draine B. T., Lee H. M., 1984, ApJ, 285, 89
Duley W. W., Williams D. A., 1981, MNRAS, 196, 269
Gilman R. C., 1969, ApJ, 155, L185
Howarth I. D., Murray J., 1991, Starlink User Note No. 50
Humphreys R. M., 1978, ApJS, 38, 309
Infrared Astronomical Satellite (IRAS) Catalogs and Atlases, Vol. 1, Explanatory Supplement, 1988, Beichman C. A., Neugebauer G., Habing H.J., Clegg P. E., Chester T. J., eds. US Government Printing Office, Washington, DC
Johnson H. L., 1966, Ann. Astrophys., 29, 525
Justtanont K., Barlow M. J., Skinner C. J., 1993, in Weinberger R., Acker A., eds, Proc. IAU Symp. 155, Planetary Nebulae. Kluwer Academic Publishers, Dordrecht, p. 341
Knacke R. F., Brooke T. Y., Joyce R. R., 1987, A&A, 187, 625
Kratschmer W., Huffman D. R., 1979, Ap&SS, 61, 195
Kwok S., Volk K. M., Hrivnak B. J., 1989, ApJ, 345, L51
Lambert D. L., Brown J. A., Hinkle K. H., Johnson H. R., 1984, ApJ, 284, 223
Léger A., Puget J. L., 1984, A&A, 137, L5
Little-Marenin I. R., Little S. J., 1990, AJ, 99, 1173 (LML)
Lloyd-Evans T., 1990, MNRAS, 243, 336
Schmidt-Kaler Th., 1982, in Schaifers K., Voigt H. H., eds, Landolt-Börnstein, Numerical Data and Functional Relationships in Science and Technology, Group VI, Astronomy, Astrophysics and Space Research, Vol. 2b. Springer-Verlag, Berlin
Sharp C. M., 1989, in Johnson H. R., Zuckerman B., eds, Evolution of Peculiar Red Giants. Cambridge University Press, Cambridge, p. 379
Skinner C. J., Whitmore B., 1987, MNRAS, 224, 335
Skinner C. J., Whitmore B., 1988a, MNRAS, 231, 169

whose silicate profile has a FWHM of 3.3 μm and shows clear evidence for additional broad components in the 11.0–11.5 and 12.7–13.2 μm regions. In this regard, S Per's silicate profile is similar to that belonging to the 'Sil$^+$' category defined by Little-Marenin & Little (1990; LML) for the *IRAS* LRS spectra of some oxygen-rich Mira variables, while the excess flux profiles of the remaining M supergiants that are brighter than 21 Jy at 12 μm are more consistent with the basic 'Sil' category of LML. The broad silicate feature associated with the fainter supergiants (Fig. 3) has some resemblance to spectra of LML's 'broad' category for Mira variables, although the M supergiant excess flux distributions peak at a shorter wavelength than the 11–12 μm quoted by LML for 'broad'-featured Miras. We note

Skinner C. J., Whitmore B., 1988b, MNRAS, 235, 603
Skinner C. J., Griffin I. P., Whitmore B., 1990, MNRAS, 243, 78
Stephens J. R., Russell R. W., 1979, ApJ, 228, 780
Tielens A. G. G. M., 1990, in Mennessier M. O., Omont A., eds,
     From Miras to Planetary Nebulae. Editions Frontières,
     Gif-sur-Yvette, p. 186

Treffers R., Cohen M., 1974, ApJ, 188, 545
White N. M., Wing R. F., 1978, ApJ, 222, 209
Willems F. J., de Jong T., 1986, ApJ, 309, L39